Chemical Geology xxx (xxxx) xxx–xxx

Contents lists available at ScienceDirect

Chemical Geology

journal homepage: www.elsevier.com/locate/chemgeo

Combining metal and nonmetal isotopic measurements in barite to identify mode of formation

Elizabeth M. Griffith[a,*], Adina Paytan[b], Ulrich G. Wortmann[c], Anton Eisenhauer[d], Howie D. Scher[e]

[a] The Ohio State University, School of Earth Sciences, 125 South Oval Mall, Columbus, OH 43210, USA
[b] University of California-Santa Cruz, Institute of Marine Sciences, 1156 High Street, Santa Cruz, CA 95064, USA
[c] University of Toronto, Department of Earth Sciences, 22 Russel St., Toronto, Ontario M5S 3B1, Canada
[d] IFM-GEOMAR, Helmholtz Centre for Ocean Research Kiel, Wischhofstrasse 1-3, D-24148 Kiel, Germany
[e] University of South Carolina, School of Earth, Ocean and Environment, Columbia, SC 29208, USA

ARTICLE INFO

Editor: Jerome G.

Keywords:
Barite
Stable strontium isotopes
Sulfidic springs
Oxygen isotopes
Sulfur isotopes
Radiogenic strontium isotopes

ABSTRACT

Barite ($BaSO_4$) is a highly stable and widely-distributed mineral found in magmatic, metamorphic, and sedimentary rocks of all ages, as well as in soils, aerosol dust, and extraterrestrial material. Barite can form in a variety of settings in the oceans (hydrothermal deposits, cold seeps, water column, or within sediments) and on the continents (soils, sulfidic springs and in the subsurface) when (1) two fluids mix – one containing barium and another containing sulfate, (2) sulfur is oxidized forming sulfate in a barium containing solution, or (3) barium or sulfate is concentrated in microenvironments where either sulfate or barium are already present. Hydrologic and biologic processes can therefore play key roles in the formation of barite and affect its geochemical composition. Characteristics of barite from various modern settings are identified here to serve as analogs for ancient systems, summarizing previous work and adding new details from the pelagic marine, hydrothermal, cold seep and continental setting. Radiogenic strontium in barite clearly identifies the source(s) of fluid forming barite with the most radiogenic values measured in continental sulfidic spring settings associated with a deep fluid component that interacts with ancient crustal rocks. Sulfur and oxygen isotopes can distinguish between sources of sulfate and identify settings where the influence of (bio)chemical processes such as sulfate reduction is prominent. There are no unique stable strontium isotopic signatures for barite formed in any of the settings investigated here, but Holocene coretop marine pelagic barite appears to have a constant offset from seawater of approximately −0.53‰ in coretop samples in contrast to the wide range of values in barite precipitated in other settings. Stable strontium mass dependent fractionation could be useful in understanding post-depositional and diagenetic processes such as authigenic precipitation and recrystallization.

1. Introduction

Barite ($BaSO_4$) is a highly stable and widely-distributed mineral found in magmatic, metamorphic, and sedimentary rocks (of all ages), as well as in soils, aerosol dust, and extraterrestrial material. Today, barite can form in a variety of settings in the oceans (hydrothermal, cold seeps, water column, sediments) and on the continents (soils, sulfidic springs and in the subsurface)– where supersaturation and precipitation of barite typically occurs from the mixing of fluids – one containing Ba and another containing sulfate (Fig. 1). In the oceans today, the global marine Ba cycle is thought to be balanced between Ba input to the oceans predominantly from rivers and groundwater (80%) and hydrothermal (20%) sources and output associated with barite and other authigenic phases (Paytan and Kastner, 1996).

Many studies of barite formation also highlight the importance of physicochemical and biochemical processes involved in the nucleation and crystal growth of barite in these settings (e.g., González-Muñoz et al., 2003; Smith et al., 2004; Sanz-Montero et al., 2009; González-Múñoz et al., 2012; Griffith and Paytan, 2012; Jennings and Driese, 2014; Widanagamage et al., 2015; Singer et al., 2016; Martinez-Ruiz et al., 2018). Barite has also been detected as a precipitate within some freshwater organisms (Finlay et al., 1983) and may be associated with agglutinated benthic foraminifera including xenophyophores (Gooday and Nott, 1982; Bertram and Cowen, 1997, 1998). The influence of

* Corresponding author.
E-mail addresses: griffith.906@osu.edu (E.M. Griffith), apaytan@ucsc.edu (A. Paytan), uli.wortmann@utoronto.ca (U.G. Wortmann), aeisenhauer@geomar.de (A. Eisenhauer), hscher@geol.sc.edu (H.D. Scher).

https://doi.org/10.1016/j.chemgeo.2018.09.031
Received 7 March 2018; Received in revised form 17 September 2018; Accepted 22 September 2018

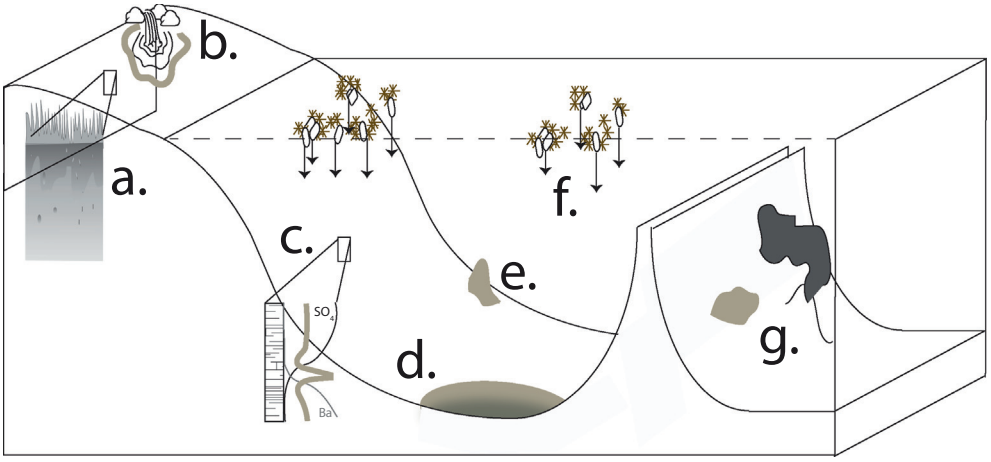

Fig. 1. Continental (a-b) and marine (c-g) settings where barite forms today. (a.) within a soil horizon; (b.) rims of sulfidic springs and along the flow path; (c.) within organic rich sediment from pore water at the boundary between the upper sulfate zone and deeper sulfate-depleted zone, where barite is remobilized and precipitated at a barite front shown in the light brown-gray peak; (d.) dissolved barium in a brine pool forms barite around its rim (light brown-gray) where it reacts with seawater sulfate; (e.) cold seeps emanating fluids enriched in Ba precipitate barite where it interacts with seawater sulfate or becomes oxidized; (f.) water column marine pelagic barite formation in decaying organic matter and is deposited in oxidized, non-sulfate reducing deep sea sediment; and (g.) black (or white) smoker hydrothermal plume with dissolved barium deposit barite at boundary between anoxic and oxic, sulfate-rich seawater (light brown-gray). (For interpretation of the references to colour in this figure legend, the reader is referred to the web version of this article.)

solution chemistry and other conditions in the environments in which barite forms on the chemical signatures recorded in barite should not be overlooked. Experimental and theoretical work, coupled with modern natural samples, provide a framework for interpreting geochemical signatures measured in modern and ancient barite samples.

The isotopic composition of some of the major nonmetal (sulfur and oxygen) and minor metal (strontium and calcium) elemental constituents of barite have been shown to be useful for identifying the origin of the solutions and processes affecting nucleation and crystal growth (Paytan et al., 2002; Griffith and Paytan, 2012 and references therein; Widanagamage et al., 2014, 2015). However, these isotope systems have not been used altogether on the same samples in a comprehensive study. In this study we suggest that the combination of multiple isotope analyses can refine environmental reconstructions.

Since barite is diagenetically stable as long as ambient sulfate is present, and oxygen isotope exchange reactions between water and sulfate are extremely slow at typical marine and subseafloor temperature and pH conditions (Kusakabe and Robinson, 1977; Zak et al., 1980; Chiba and Sakai, 1985), it is generally assumed that sulfur and oxygen isotopic signatures ($\delta^{34}S$, $\delta^{18}O$) in barite record the isotopic ratios of sulfate at the time of barite formation. While sulfate does not exchange isotopes with ambient water under normal marine pressure, temperature, and pH conditions, microbially mediated reduction/oxidation and isotope exchange reactions, as well as by abiotic re-oxidation of reduced sulfur species, will affect dissolved sulfate in interstitial waters (e.g., Chiba and Sakai, 1985; Brunner and Bernasconi, 2005; Brunner et al., 2005; Wortmann et al., 2007) and these isotopic signatures are recorded in barite formed from these solutions. Radiogenic strontium ratios ($^{87}Sr/^{86}Sr$) are indicative of the origin or source of solutions for barite precipitation (Reesman, 1968; Maynard et al., 1995; Paytan et al., 2002). Mass dependent stable strontium and calcium isotopic fractionation ($\delta^{88/86}Sr$, $\delta^{44/40}Ca$) in barite appear to be influenced by chemical kinetic effects during crystal growth (Griffith et al., 2008; Widanagamage et al., 2014) which can occur post-deposition during diagenesis or during authigenic precipitation of barite.

We combine new and previously published results from radiogenic $^{87}Sr/^{86}Sr$ ratios and stable Sr-isotope measurements ($\delta^{88/86}Sr$), along with $\delta^{34}S$ and $\delta^{18}O$ measurements of modern barite samples of marine (pelagic, hydrothermal, and cold seep deposits) and non-marine (continental surficial sulfidic spring deposits and soils) origin to demonstrate the usefulness of measuring multiple metal and nonmetal isotopes to identify modes of barite formation. These relationships in modern settings can serve as analogs for ancient barite deposits, expanding existing geochemical methods to understand their genesis (e.g., Koski and Hein, 2003; Torres et al., 2003).

2. Methods

2.1. Barite extraction

Samples were confirmed to be of sufficient purity for bulk dissolution and isotopic analysis by scanning electron microscopy (SEM) with energy-dispersive spectrometry (EDS) prior to analysis. Samples less than ~90% barite (i.e., the Holocene coretop marine pelagic barite and continental surficial sulfidic spring deposits) were separated from contaminating material using a procedure modified from Paytan et al. (1993).

2.2. Sulfur isotope analysis

Sulfur (S) isotope analyses were done by continuous-flow mass spectrometry using a Carlo ErbaNA 1500 elemental analyzer connected to a Micromass Isoprime mass spectrometer at the U.S. Geological Survey, Menlo Park (indicated in Table 1). Samples of 4–8 mg were introduced in tin boats with 5 mg vanadium pentoxide (V_2O_5) mixed in with each sample. A commercial tank of SO_2 was used as a reference gas for $\delta^{34}S$ measurements, and results are reported relative to the Vienna Canyon Diablo Troilite (VCDT) standard, with a standard deviation (1σ) of 0.15‰ based on repeat analyses of NBS 127.

Additional S isotopes were measured at the University of Toronto, about 200 µg of powdered barite samples are mixed with ~600 µg of vanadium pentoxide (V_2O_5) and sealed into a tin cup. This cup is introduced into Elemental Analyzer system (Eurovector 3000), and flash combusted at 1700 °C under oxygen atmosphere. The evolving SO_2 is routed into our continuous flow isotope ratio monitoring mass spectrometry system (CFIRM-MS, see above), which measures the relative abundances of ^{34}S versus ^{32}S. We express the results in the usual delta notation relative to VCDT.

The CFIRM-MS system is calibrated using the following international sulfate standards NBS 127, IAEA SO5 and IAEA SO6 (21.1‰, +0.49‰, and −34.05‰, VCDT respectively; Coplen et al., 2001). We additionally use an in-house synthetic $BaSO_4$ (Sigma-Aldrich) standard (8.6‰, VCDT) to test for drift and memory effects. Repeated measurements of the in-house standard (typically > 10 measurements per run) and international standards (3–4 measurements per run) yield an average reproducibility of 0.15‰ (1σ).

2.3. Oxygen isotope analysis

Oxygen isotopic analyses were measured at the University of Toronto (indicated in Table 1). For oxygen isotope measurements,

Table 1
Isotopic compositions of barite samples.

Name	$\delta^{88/86}Sr$	error	$^{87}Sr/^{86}Sr$	Error		$\delta^{34}S$	Error		$\delta^{18}O$	Error	
	NBS-987	[2SD]		[2SD]		CDT	[1SD]		VSMOW	[1SD]	
Holocene core top marine (pelagic) barite											
VNTR01 8PC, 0.0 N, 110.5 W, 3791 mbsl	−0.12	0.02	0.70916	0.000013	This study[K]						
PLDS-069PC, 0–5, 1.0 N, 105.6 W, 3527 mbsl	−0.16	0.01	0.70910	0.000004	This study[K]						
TN057-1, 0–5, 47.1 S, 5.9 E, 4398 mbsl	−0.16	0.01	0.70917	0.000004	This study[K]						
Average and SD:	−0.14	0.02	0.70914	0.00004		21.05	0.21	n = 13; Paytan et al. (1998); Markovic et al. (2016)	5.84	0.41	n = 10; Markovic et al. (2016)
Hydrothermal (oceanic) barite											
Juan de Fuca, exterior chimney, Middle Valley	0.01	0.01	0.70451	0.000004	This study[K]	20		Estimate from Paytan et al. (2002)	13		ave. Brent Hill barite in Middle Valley (Goodfellow et al., 1993)
Replicate (JdFR ALV 2254–22)	0.02	0.00	0.70441	0.000002	This study[K]						
JdF Middle Valley 2254 23–1 ext. chim	0.03	0.10	0.70448	0.000018	This study[C]	22.94	#	This study[T]	9.06	##	This study[T]
Duplicate						19.7	#	Paytan et al. (2002)			
JdF Middle Valley 2254 28–1	0.05	0.05	0.70444	0.000013	This study[C]	22.68	0.04	This study[T]	8.86	##	This study[T]
JdF South Explorer Ridge ALV 1459–8			0.70535	#	Paytan et al. (2002)	20.8	#	Paytan et al. (2002)			
Duplicate						22.93	0.17	This study[T]	9.43	##	This study[T]
JdF Axial Seamount ALV 2084-2A-1 Casm Site			0.70625	#	Paytan et al. (2002)	19.5	#	Paytan et al. (2002)	6.52	##	This study[T]
Mid Atlantic Ridge Lucky Strike, chimney barite	−0.13	0.01	0.70516	0.000006	This study[K]	21		Estimate from Paytan et al. (2002)			
Replicate	−0.14	0.00	0.70517	0.000000	This study[K]						
Guaymas Basin (GB1) 1173–1	−0.09	0.07	0.70615	0.000012	This study[C]	26.4	#	Paytan et al. (2002)			
Guaymas Basin (GB2) 1173–11	−0.06	0.02	0.70565	0.000016	This study[C]	22.51	#	This study[T]	8.74	0.10	This study[T]
Duplicate						23.2	#	Paytan et al. (2002)			
Average and SD:	−0.04	0.08	0.70516	0.00070		21.8	2.1		9.3	2.1	
Other barite: cold seep (oceanic), subsurface/diagenetic											
San Clemente Basin	−0.08	0.00	0.70868	0.000001	This study[K]	24		ave. from Paytan et al. (2002)			
San Clemente Canyon	−0.06	0.06	0.70886	0.000009	This study[C]	21.93	#	This study[T]	9.81	0.08	This study[T]
Baja Ensenada dredged	−0.04	0.06	0.70870	0.000009	This study[C]	29.56	0.10	This study[T]	13.74	0.20	This study[T]
765C 34–2, 118–121 cm			0.71082	#	Paytan et al. (2002)	23.7	#	Paytan et al. (2002)	4.66	##	This study[T]
Average and SD:	−0.06	0.02	0.70926	0.00104		24.7	3.4		9.4	4.6	
Continental barite: warm, hot spring deposits											
Zodletone Spring, OK, crust on spring (OK/S6)	0.13	0.08	0.71025	0.000011	Widanagamage et al. (2015)	33.4	#	This study[M]	2.98	##	This study[T]
Zodletone Spring, OK, end of drainage (OK/S1)	0.12	0.05	0.71027	0.000023	Widanagamage et al. (2015)	35.9	#	This study[M]	8.33	##	This study[T]
Stinking Creek, OK (OK/S7)	0.16	0.02	0.71013	0.000003	Widanagamage et al. (2015)	42.4	#	This study[M]	10.56	##	This study[T]
Duplicate						42.1	#	This study[M]			
Stinking Creek, rock sample from bank (OK/LB)						32.6	#	This study[M]	8.38	##	This study[T]
Stinking Spring, UT: lower terrace (UT/S6)	−0.43	na	0.71720	na	Widanagamage et al. (2015)						
Stinking Spring, UT: lower terrace (UT/S7)	−0.30	0.03	0.71709	0.000009	Widanagamage et al. (2015)	32.1	#	This study[M]	3.39	##	This study[T]
Stinking Spring, UT: lower terrace (UT/S8)	−0.19	0.06	0.71723	0.000017	Widanagamage et al. (2015)	35.6	#	This study[M]	1.89	##	This study[T]
Duplicate						37.8	#	This study[M]	2.07	##	This study[TR]
Triplicate									1.98	##	This study[TR]

(*continued on next page*)

Table 1 (*continued*)

Name	$\delta^{88/86}$Sr	error	^{87}Sr/^{86}Sr	Error		δ^{34}S	Error		δ^{18}O	Error	
	NBS-987	[2SD]		[2SD]		CDT	[1SD]		VSMOW	[1SD]	
Stinking Spring, UT rock sample (UT/Liz1)	−0.21	0.02	0.71743	0.000007	This study[C]	31.6	#	This study[M]	4.25	##	This study[T]
Stinking Spring, UT rock sample (UT/Liz2)	−0.45	0.10	0.71720	0.000012	This study[C]						
Doughty Springs, CO: Middle Spring (CO/M)	0.08	0.02	0.71354	0.000016	Widanagamage et al. (2015)	31.9	#	This study[M]	2.61	##	This study[TR]
Duplicate									2.80	##	This study[T]
Doughty Springs, CO: Middle Spring (CO/ME)	0.07	0.07	0.71361	0.000002	Widanagamage et al. (2015)	31.7	#	This study[M]	3.63	##	This study[TR]
Duplicate									3.74	##	This study[T]
Doughty Springs, CO: Middle Spring (CO/ME1)	0.06	0.05	0.71364	0.000023	Widanagamage et al. (2015)	27.7	#	This study[M]	−0.99	##	This study[TR]
Duplicate									−0.72	##	This study[T]
Doughty Springs, CO: Middle Spring (CO/ME2)	0.05	0.04	0.71362	0.000021	Widanagamage et al. (2015)	31.5	#	This study[M]	1.51	##	This study[T]
Duplicate						32.6	#	This study[M]			
Doughty Springs, CO: Middle Spring (CO/ME3)	−0.06	0.06	0.71371	0.000016	Widanagamage et al. (2015)	30.9	#	This study[M]	2.22	##	This study[T]
Duplicate						31.4	#	This study[M]			
Doughty Springs, CO: Middle Spring (CO/ME4)	0.03	0.04	0.71365	0.000015	Widanagamage et al. (2015)	31.1	#	This study[M]	1.04	##	This study[T]
Doughty Springs, CO: Drinking Spring (CO/D2)	0.05	0.04	0.71348	0.000015	Widanagamage et al. (2015)	23.1	#	This study[M]	0.77	##	This study[TR]
Duplicate									0.44	##	This study[T]
Doughty Springs, CO: Bathtub Spring (CO/B2)	−0.06	0.03	0.71346	0.000025	Widanagamage et al. (2015)	21.3	#	This study[M]	−2.42	##	This study[T]
Average and SD:	−0.06	0.20	0.71409	0.00254		32.5	5.2		2.8	3.1	

K = $\delta^{88/86}$Sr and ^{87}Sr/^{86}Sr data from IFM-GEOMAR.
C = $\delta^{88/86}$Sr and ^{87}Sr/^{86}Sr data from Univ of South Carolina.
T = δ^{34}S or δ^{18}O from University of Toronto.
TR = δ^{34}S from University of Toronto after reprecipitation (see Methods).
M = δ^{34}S from U.S. Geological Survey.
# = external precision for Paytan et al. (2002) ^{87}Sr/^{86}Sr = ± 0.000 02; δ^{34}S standard deviation for CDT 1 sigma = ± 0.15‰.
= δ^{18}O standard deviation on international standards = ± 0.2‰ at Univ. of Toronto.
ave. = average.
SD = standard deviation.

Table 2
Barite formation setting and general characteristics.

	Oceanic			Continental		Other: subsurface/ diagenetic
	Hydrothermal	Cold seep	Pelagic marine	Spring	Soil	
$BaSO_4$ content	< 50% to > 90%	< 50% to > 90%	< 10%	< 50% to > 90%	> 90% in small areas	< 50% to > 90%
Sr content	Up to 5 wt%	Up to 5 wt%	Up to 3 wt%	Up to 5 wt%	Up to 10 wt%; most "little" Sr	Not determined
Crystal size and form	Coarse grained (up to 2 cm), euhedral, rosette	20–700 um, bladed, rosette	< 20 um, ovoid or microcrystalline	< 1 mm, intergrown, tabular, needles, asters	Sub-mm prismatic, tabular; coarse grained (> 10 mm)	< 1 mm, needles, bladed, tabular
Associated megafauna? Other associations?	Yes	Yes	No	No; various filamentous microfossils, cemented debris, stromatolitic	No; root channels	No
$\delta^{34}S$	Seawater[a] to ≫seawater[a]	Seawater[a] to ≫seawater[a]	Seawater[a]	Varies with source and process	Varies with source (≪seawater[a]) and process	Seawater[a] to ≫seawater[a]
$\delta^{18}O$	Seawater[a] to ≫seawater[a]	Seawater[a] to ≫seawater[a]	Seawater[a] to < seawater[a]	Varies with source (≪seawater[a]) and process	Varies with source and process	Seawater[a] to > > seawater[a]
$^{87}Sr/^{86}Sr$	< Seawater[a]	< Seawater[a] to > seawater[a]	Seawater[a]	Seawater[a] to ≫seawater[a]	Not determined	< Seawater[a] to > seawater[a]
$\delta^{88/86}Sr$	Variable ≪ seawater[a]	≪Seawater[a]	Constant offset ≪ seawater[a]	Variable	Not determined	≪Seawater[a]

[a] Seawater indicates contemporaneous seawater at time of formation; modern seawater $\delta^{34}S_{SO4}$ = 21.15‰ ± 0.15, $\delta^{18}O_{SO4}$ = 8.67‰ ± 0.21 (1σ; Johnston et al., 2014), $^{87}Sr/^{86}Sr$ = 0.709175 (e.g., Paytan et al., 1993), $\delta^{88/86}Sr$ = 0.39‰ (e.g., Pearce et al., 2015).

about 200 μg powdered barite was measured into a silver capsule. Using a helium atmosphere, this capsule is pyrolized in a high temperature furnace (Hekatech HT EA) at 1350 °C. The evolved CO was routed through an Ascarite trap, separated on a Molsieve 5A, and subsequently introduced via an open split interface (Finnigan Conflo III) into a continuous flow isotope ratio monitoring mass spectrometry system (CFIRM-MS, Finnigan MAT 253). The resulting relative abundances of ^{18}O versus ^{16}O are expressed in delta notation relative to VSMOW (Vienna Standard Mean Ocean Water).

We calibrate our measurements using the following international sulfate standards NBS 127 (+8.6‰ VSMOW, IAEA SO5 + 12.13‰ VSMOW and IAEA SO6–11.35‰ VSMOW, USGS 32 + 25.4‰ VSMOW; Coplen et al., 2001; Böhlke et al., 2003; Brand et al., 2009). We additionally use an in-house synthetic BaSO4 standard (Sigma-Aldrich, 11.9 ± 0.2‰ VSMOW) to test for instrument drift and memory effects. Repeated measurements of the in-house standard (typically > 10 per run) and international standards (3–4 standards per run) yield a reproducibility of ± 0.2‰ (1σ). Five samples were dissolved and re-precipitated prior to analysis to eliminate any potential influence of non-barite components following Breit et al. (1985), see Table 1.

2.4. Strontium isotope analysis

Barite samples were dissolved for Sr isotope analysis using cation exchange resin as a chelation agent following previous work by Paytan et al. (1993). The Sr fraction was separated using Eichrom Sr Spec resin prior to analysis on either the Neptune Plus multicollector-inductively coupled mass spectrometer (MC-ICPMS) at the University of South Carolina or the Triton thermal ionization mass spectrometer (TIMS) at IFM-GEOMAR as indicated in Table 1. Measurements of $^{87}Sr/^{86}Sr$ on the MC-ICPMS had an external precision of better than ± 0.000015 determined by triplicate analyses of samples. Measurements of $^{87}Sr/^{86}Sr$ on the TIMS had an external precision of ± 0.000009 determined by repeat analyses of IAPSO seawater (n = 10). During analysis, the mean $^{87}Sr/^{86}Sr$ ratio of IAPSO seawater was 0.709169 (n = 6) and 0.709168 (n = 10) on the MC-ICPMS and TIMS respectively.

The MC-ICPMS detects simultaneously masses required to measure both radiogenic and stable isotopic composition of Sr, with mass discrimination within the instrument corrected using internal and external corrections following Scher et al. (2014). Conventional internal correction was done assuming non-radiogenic $^{86}Sr/^{88}Sr$ = 0.1194 to calculate radiogenic $^{87}Sr/^{86}Sr$ (Nier, 1938). Samples and standards were doped with 20 ppb Zr for the external mass bias correction using masses 90 and 91 (i.e., ^{90}Zr and ^{91}Zr). Isobaric interferences of krypton (Kr) on masses 84 and 86 and rubidium (Rb) on mass 87 can result from trace quantities of Kr in the argon supply and incomplete separation of Rb from Sr, therefore masses 82, 83, and 85 (i.e., ^{82}Kr, ^{83}Kr, ^{85}Rb) were measured to correct for these interferences. The sample standard bracketing technique was used to constrain further mass bias during analyses, improving the reproducibility of the measurements (e.g., Kramchaninov et al., 2012; Scher et al., 2014). Typical procedural blanks are < 0.1% of Sr in the processed barite, sufficiently low for the sample size prepared (Widanagamage et al., 2015). During analysis, the mean $\delta^{88/86}Sr$ of seawater was 0.35‰ (2SD = 0.08‰; n = 6) and NIST SRM 987 was 0.00‰ (2SD = 0.07‰; n ≥ 47).

Stable Sr isotope measurements on the TIMS were done following Krabbenhöft et al. (2009) and AlKhatib and Eisenhauer (2017). In summary, the dissolved barite sample is split into two aliquots: one aliquot is spiked using a mixed ^{87}Sr—^{84}Sr double spike and one aliquot is unspiked (used to measure the sample $^{87}Sr/^{86}Sr$). The Sr splits of the two aliquots are separated independently using extraction chromatography (Eichrom Sr-Spec resin). The Sr splits are dried down and treated with nitric and H_2O_2 to remove organic matter that elutes from the resin and impacts beam stability. About 500 ng of Sr is loaded onto rhenium filaments along with 1 μl of 1 M phosphoric acid and 1 μl of tantalum activator and analyzed using TIMS. Typical procedural blanks

are < 1 ng of Sr, sufficiently low for the sample size prepared. The mean $\delta^{88/86}$Sr of seawater is 0.391‰ (2× standard error of the mean (2SEM) = 0.004‰; n = 63) and JCP-1 coral standard is 0.195‰ (2SEM = 0.03‰; n = 87) as reported in AlKhatib and Eisenhauer (2017).

3. Results and discussion

General characteristics of different barite formation settings from the literature and this work are summarized in Table 2 and detailed below. The settings with the highest barite content include some hydrothermal and cold seep marine settings, some springs and soil samples, and other subsurface and diagenetic settings, however the barite in these settings is spatially restricted to the formation site. Barite formed in soils appear to have the highest concentrations of Sr, while pelagic marine barite has typically the lowest Sr content. The smallest barite crystals (typically < 20 μm and between 1 and 5 μm). The radiogenic Sr in pelagic barite records the seawater Sr curve. Radiogenic Sr isotopes in barite in continental settings are often very different from contemporaneous seawater values, tending towards much more radiogenic values. Stable Sr isotopic compositions are variable in all settings expect for marine pelagic barite. Generally, the stable Sr isotopic composition of barite is more negative than contemporaneous seawater Sr due to mass dependent isotopic fractionation of Sr incorporated in barite. The only settings with known associations with megafauna are in hydrothermal and cold seep marine settings, although association with various filamentous microbes occur in continental spring settings. Sulfur and oxygen isotopes in the marine setting are equivalent to contemporaneous sulfate in seawater while in the subsurface diagenetic settings they are typically heavier. Sulfur and oxygen isotopes in barite from continental settings can be quite different from contemporaneous seawater sulfate.

3.1. Sulfur isotopes

The sulfur isotopic composition of barite samples exhibits a very large range of δ^{34}S values. Cold seep and other types of barite precipitated in the marine environment including diagenetic barite (e.g., barite that forms from pore fluids in marine sediments at an oxic-anoxic boundary post deposition) have δ^{34}S that range from seawater-like values of 21‰ to > 80‰ as seen in Fig. 2a (see also Aquilina et al., 1997; Greinert et al., 2002; Paytan et al., 2002; Feng and Roberts, 2011; Stevens et al., 2015). The samples with elevated δ^{34}S precipitated from sulfate in fluids that have undergone varying degrees of microbial sulfate reduction either by dissimilatory sulfate reduction or anaerobic oxidation of methane associated with sulfate reduction (e.g., Harrison and Thode, 1958; Deusner et al., 2014).

The S isotopic fractionation (or shift in δ^{34}S) imparted during microbial sulfate reduction varies between a few ‰ up to 70‰ (Wortmann et al., 2001). The expression of this isotopic fractionation depends chiefly on the sulfate reduction rate (Rees, 1973; Wing and Halevy, 2014) and the sulfate concentration (Seal et al., 2000). The effect of microbial sulfate reduction on the S-isotope ratio of the ambient water from which the barite forms depends on the relative ratios of the sulfate reduction flux versus the mixing rate with unmodified water. These diverse factors contribute to the variable degree of enrichment seen in the barite δ^{34}S values relative to seawater or other solutions from which barite precipitated.

The marine sulfate sulfur isotopic composition (present-day δ^{34}S = 21.5‰; Johnston et al., 2014) reflects the balance of sulfide and sulfate input and removal from the oceans and their isotopic compositions (Wortmann and Paytan, 2012). Pelagic marine barite records seawater sulfate δ^{34}S with little isotopic offset (< 0.4‰; Paytan et al., 1998) and has been useful in reconstructing seawater sulfate δ^{34}S through time (e.g., Paytan et al., 1998, 2004). For the Phanerozoic, seawater sulfate δ^{34}S ranged from around +38‰ to +10‰ (see Gill et al., 2007 and references therein). For the Cenozoic, the range was much smaller, only around 6‰ between 16‰ and 22‰ (Paytan et al., 1998).

Marine hydrothermal barite δ^{34}S typically falls well below contemporaneous seawater sulfate δ^{34}S due to mixing of sulfate of hydrothermal origin, produced by oxidation of hydrogen sulfide in hydrothermal fluids a process associated with little to no isotopic fractionation (Hannington and Scott, 1988; Seal et al., 2000). The samples from the Guaymas Basin hydrothermal vent area in the Gulf of California have δ^{34}S values higher than seawater (and hydrothermal sulfide) likely due to sulfate from fluids modified when they move through the sediment-covered ridge system where microbial sulfate reduction removes preferentially the light S isotopes as previously described by Paytan et al. (2002) following work by Elsgaard et al. (1994).

Pedogenic barite in an acid-sulfate soil (Lufkin Series in south-central Texas, USA) has δ^{34}S values higher than jarosite ($KFe_3{}^{+3}(OH)_6(SO4)_2$) which was found to be the most likely source of S during reducing, inundated, wet conditions deep within the soil (average jarosite δ^{34}S = −12.6‰; Jennings and Driese, 2014). Jennings and Driese (2014) suggest that alternating wet/dry conditions produce changing redox conditions resulting in sulfur-reducing and -oxidizing microbial cycling, with a significant isotopic imprint on the precipitated pedogenic barite due to the large isotopic effects of sulfur-reducing bacteria. This could explain the increase in pedogenic barite δ^{34}S values to +5.5‰ which is > 18‰ higher than the jarosite value (Fig. 2a). Nonetheless, these barite samples exhibit the lowest δ^{34}S values measured in barite samples formed today or in the recent past due to their S source with characteristically low δ^{34}S values.

Continental barites precipitated in or near a sulfidic spring in Oklahoma measured in this study have δ^{34}S values that are also higher than the sulfide emanating from the spring by 6 to 15‰ (spring source δ^{34}S = +27.1‰; Senko et al., 2004) as measured in the barite crust around the spring source and in the adjacent creek, respectively. Previous work concluded that anaerobic, anoxygenic, phototrophic bacteria play a dominant role in oxidizing sulfide to sulfate in the spring (Senko et al., 2004). However, S isotopic fractionation measured in laboratory bacterial experiments show negligible to very small shifts to lower values (−2.3 to −0.7‰) during S oxidation, depending on bacterial and chemical conditions (Brabec et al., 2012). Therefore, the elevated values of δ^{34}S in barite cannot be the result of S oxidation but must be the result of mixing of various sulfate sources to different degrees resulting in elevated values in barite. Isotopic composition of upcreek sulfate (+8.4‰) is consistent with sulfate in nearby Permian evaporite beds (Senko et al., 2004) and is one potential source. Dissolved sulfate measured where the spring drainage reaches the creek was 10.4‰, representing a mixture of spring and creek isotopic compositions (Senko et al., 2004). However, the separated barites measured in this study clearly have the highest δ^{34}S values.

Therefore, we suggest that this is evidence for more complex sulfur cycling in the spring sediment at the site in Oklahoma. The S isotopic composition of the barite provides evidence of sulfate reduction, resulting in isotopically heavier sulfate where the barite precipitates. Sulfate-reduction activity has been detected at the site associated with phototrophic mats (Elshahed et al., 2003). The isotopic effect of sulfate reduction would likely be greater where sulfate concentrations are higher, further from the spring. Furthermore, lower sulfate reduction rates have been shown to have larger isotopic fractionations (Aharon and Fu, 2000) resulting in a stronger influence on the barite δ^{34}S than would be expected based on the cycling of sulfur. Other hydrogeochemical differences between the high dissolved solids in the spring water and the freshwater creek can also influence the observed isotopic offsets between barite and dissolved sulfate.

The other continental sulfidic spring sites measured in this study show less variation in δ^{34}S (< 6‰ within any of the springs, Table 1). It is possible that the barites in the other sites are recording (1) the

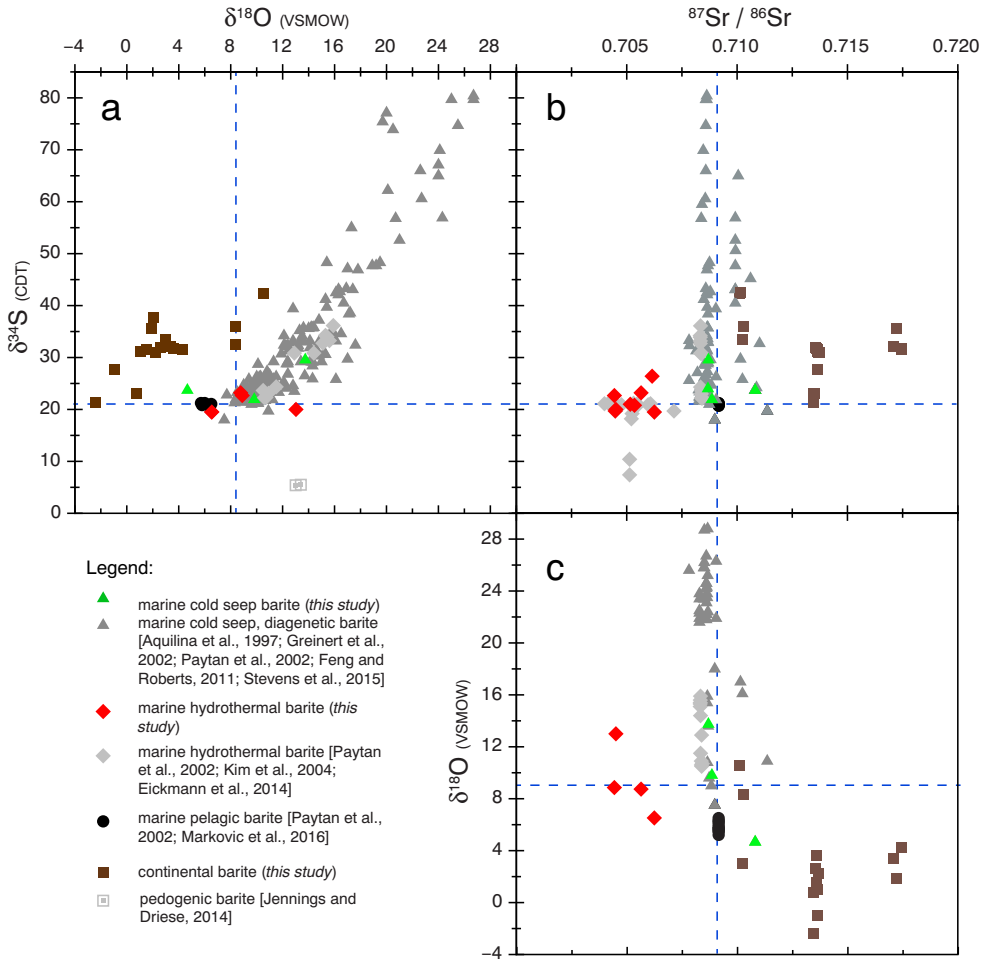

Fig. 2. (a.) Stable sulfur ($\delta^{34}S$ in ‰ relative to CDT) and oxygen ($\delta^{18}O$ in ‰ relative to VSMOW) isotopic composition of barite. Radiogenic strontium ($^{87}Sr/^{86}Sr$) isotopic composition of barite versus (b.) $\delta^{34}S$ and (c.) $\delta^{18}O$. Published data plotted include: marine cold seep and diagenetic barite data from [Aquilina et al., 1997; Greinert et al., 2002; Paytan et al., 2002; Feng and Roberts, 2011; Stevens et al., 2015], marine hydrothermal barite data from [Paytan et al., 2002; Kim et al., 2004; Eickmann et al., 2014], marine pelagic barite data from [Paytan et al., 2002; Markovic et al., 2016], and pedogenic barite data from [Jennings and Driese, 2014]. Dashed blue lines indicate isotopic composition of modern seawater sulfate ($\delta^{34}S$ and $\delta^{18}O$) and dissolved strontium ($^{87}Sr/^{86}Sr$) from [Johnston et al., 2014; Paytan et al., 1993].

isotopic composition of the sulfide in springs, (2) some mixture of S from different sources at the locations, or (3) S cycling within the system including oxidation and reduction, but to a lesser extent than seen in Oklahoma. Additional information such as the spring sulfide $\delta^{34}S$ and dissolved sulfate $\delta^{34}S$ in the spring water and along the creek would be required to differentiate between these sources and processes influencing their S isotopic composition and that recorded in barite obtained from sediments and crusts. In some cases, it is possible to use additional isotope systems, like oxygen isotopes described below, to distinguish between these sources and processes (Table 2, see discussion below).

3.2. Oxygen isotopes

The largest range of measured values of oxygen isotopes in barite has been recorded in the detailed work of previous studies of marine cold seeps (Aquilina et al., 1997; Greinert et al., 2002; Feng and Roberts, 2011; Stevens et al., 2015). Most of the previous measurements of barite from marine cold seeps have $\delta^{18}O$ values greater than seawater sulfate $\delta^{18}O$, indicating the importance of biological sulfate reduction in the crusts or sediment driving both the sulfur and oxygen isotopic composition of the residual sulfate to higher values (Seal et al., 2000). Diagenetic barite from Ocean Drilling Program Site 765 has the lowest $\delta^{18}O$ value (4.66‰; Table 1) suggesting it may have precipitated from pore-fluids which differ in their chemistry from present day seawater (Fig. 2c; Paytan et al., 2002). As previously mentioned additional isotope systems could shed light on the pore-water source (Table 2). Indeed, relatively high $^{87}Sr/^{86}Sr$ indicate the presence of fluid impacted by terrigenous material (see below).

Marine pelagic barite $\delta^{18}O$ has been measured and reported using different methods of purification from deep sea sediment (Turchyn and Schrag, 2004; Markovic et al., 2016). We report and discuss briefly the more recent data from Markovic et al. (2016), which shows an offset of 2.0 to 2.5‰ in marine pelagic barite towards lower values when compare to seawater sulfate $\delta^{18}O$ (~8.6‰; Johnston et al., 2014). It was suggested that this lower value (Figs. 2, 3) is a result of incorporation of sulfate from oxidized organic S compounds within sinking and decaying organic matter where marine pelagic barite forms (Markovic et al., 2016). Organic S compounds should have $\delta^{34}S$ values close to seawater sulfate, however oxygen from seawater can be incorporated into sulfate during oxidation of organic S compounds shifting the barite formed from this sulfate towards lower values (seawater is 0‰ VSMOW), see discussion in Markovic et al. (2016).

Due to methodological differences involved in purifying marine pelagic barite which may alter the original seawater sulfate $\delta^{18}O$ signature recorded in barite, it is unclear at this time how exactly seawater sulfate $\delta^{18}O$ has varied over the Cenozoic but compared to sulfate $\delta^{34}S$ there are considerably more variations in sulfate $\delta^{18}O$ fluctuating by several permil (Turchyn and Schrag, 2004, 2006; Markovic et al., 2016). It is generally believed that these fluctuations are related to change in global shelf area (Turchyn and Schrag, 2006; Markovic et al., 2016). Because of the slow kinetics of isotopic exchange reactions between oxygen in sulfate and water at typical seawater temperature and pH conditions (Chiba and Sakai, 1985) and the long residence time of sulfate in the ocean, seawater sulfate $\delta^{18}O$ reflects the balance of sulfate sources (weathered evaporites and oxidative pyrite weathering), sulfate sinks (e.g., evaporite and pyrite burial), and cycling of sulfate within the ocean (e.g., sulfate reduction and sulfide oxidation) (Claypool et al.,

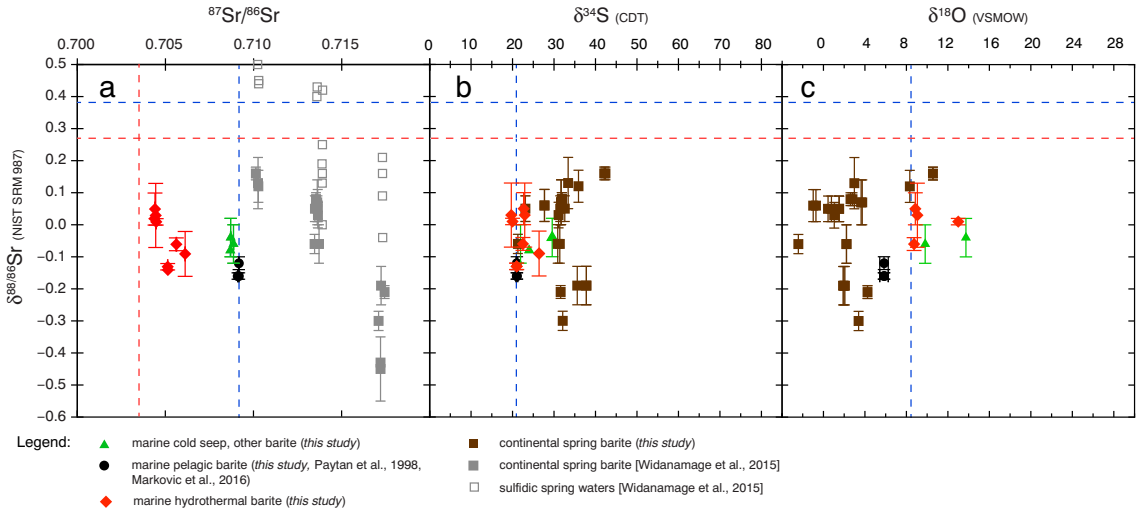

Fig. 3. (a.) Radiogenic ($^{87}Sr/^{86}Sr$) and stable ($\delta^{88/86}Sr$ in ‰ relative to NIST SRM 987) Sr isotopic composition of samples of barite (solid symbols) and some waters (open symbols). Stable Sr ($\delta^{88/86}Sr$) versus (b.) $\delta^{34}S$ and (c.) $\delta^{18}O$. See legend for sources of data. Dashed lines indicate isotopic composition of modern seawater sulfate in blue ($\delta^{34}S$ and $\delta^{18}O$) and dissolved hydrothermal Sr in red and seawater Sr in blue ($^{87}Sr/^{86}Sr$ and $\delta^{88/86}Sr$) from (Paytan et al., 1993; Fietzke and Eisenhauer, 2006; Krabbenhöft et al., 2010; Johnston et al., 2014; Pearce et al., 2015).

1980). Data over the Phanerozoic obtained from evaporites demonstrate that seawater sulfate $\delta^{18}O$ was not higher by > 10‰ relative to today's value (e.g., Claypool et al., 1980).

New data from this study show some marine hydrothermal barite samples can have similar $\delta^{18}O$ values to pelagic and other barite formed in the marine setting (Figs. 2, 3). Marine hydrothermal barite samples also exhibit some values higher than contemporaneous seawater sulfate $\delta^{18}O$ pointing to the potential importance of biological sulfate reduction in this setting.

Pedogenic barite from the Lufkin Series in south-central Texas, USA has slightly higher $\delta^{18}O$ values than the measured exchangeable sulfate, gypsum and jarosite in barite-bearing soil profiles (~3‰ higher), but > 10‰ higher than meteoric water (~10‰ higher than groundwater) (Jennings and Driese, 2014). Together with sulfur isotope data, it was suggested that the source of sulfate in pedogenic barite at this location is from mineral dissolution with slight enrichments in oxygen (and sulfur) isotopes due to microbial sulfate reduction (Jennings and Driese, 2014), which increases both $\delta^{34}S$ and $\delta^{18}O$ of the residual sulfate.

Unlike the pedogenic barite, the source of oxygen is sulfate in the continental sulfidic spring setting measured in this study is likely not dominated by mineral dissolution but originates from water. Previous work concluded that anaerobic, anoxygenic, phototrophic bacteria play a dominant role in oxidizing sulfide to sulfate at the sulfidic spring in Oklahoma (Senko et al., 2004). Oxidation of sulfur this way results in an oxygen isotopic composition of the sulfate derived completely from oxygen in water. Furthermore, sulfate $\delta^{18}O$ can change due to equilibrium exchange reactions and/or kinetic effects during sulfate reduction and/or disproportionation, as well as the uptake of ambient $\delta^{18}O$ during abiotic oxidation (Taylor et al., 1984; Fritz et al., 1989; Van Stempvoort and Krouse, 1994; Böttcher et al., 2001a, 2001b, 2005; Brunner et al., 2005; Wortmann et al., 2007; Turchyn et al., 2010; Balci et al., 2012; Antler et al., 2013). Incorporation of some oxygen from air (+23‰; Kroopnick and Craig, 1972) would also drive the oxygen isotopic composition of the barite sulfate to higher values.

Additional data on the $\delta^{18}O$ of the water or dissolved sulfate is not available at any of these continental sulfidic spring sites to confirm the exact origin of $\delta^{18}O$ in these barite samples. The values are much lower than expected if air was the source of oxygen during aerobic oxidation of sulfide. Weathered evaporites (Permian evaporite beds ~10‰; Claypool et al., 1980) could provide a source of sulfate and influence the $\delta^{18}O$ in sulfate in the spring drainage and creek in Oklahoma and would be consistent with the sulfur isotope data at this site. The barite crust on the spring has a $\delta^{18}O$ value of 3‰ much lower than the dissolved sulfate in the drainage (8‰) and creek (~10‰) suggesting anoxygenic, phototrophic oxidation of sulfide by bacteria dominates at the location of the spring while additional source(s) of sulfate are likely present along the drainage and creek. A low $\delta^{18}O$ value for the spring water is expected if the water emanating from the sulfidic springs originates from recirculated meteoric water. All the other sulfidic spring sites we sampled have low barite $\delta^{18}O$ (< 4.25‰) most likely imparted by low meteoric water $\delta^{18}O$ values expected for their continental interior setting (Dansgaard, 1964; Bowen and Revenaugh, 2003). The lowest barite $\delta^{18}O$ values measured here are all found in samples from continental sulfidic spring settings (Figs. 2, 3).

3.3. Radiogenic strontium

When plotted with their respective $^{87}Sr/^{86}Sr$ values (Fig. 2c), the various types of barite can be distinguished. Hydrothermal barites range from near hydrothermal fluid values of relatively unradiogenic $^{87}Sr/^{86}Sr$ to near modern seawater values depending on the contribution of seawater to their formation. Similarly, cold seep barites are typically only slightly offset from modern seawater (and marine pelagic barite) due to limited contribution of unradiogenic Sr from the oceanic crust (and presumably other dissolved ions) relative to seawater contribution during formation. Some continental fluids also have overlapping $^{87}Sr/^{86}Sr$ values with seawater hence barite from continental settings (e.g., within the Peru Margin; Aquilina et al., 1997) may also have similar $^{87}Sr/^{86}Sr$ values to Holocene marine pelagic barite. Over the Phanerozoic, seawater $^{87}Sr/^{86}Sr$ has varied relatively little (~0.003; Veizer et al., 1999) compared to the variations we see between marine settings and continental sulfidic spring barite (Figs. 2, 3). The extremely high $^{87}Sr/^{86}Sr$ values of the continental spring settings in Utah and Colorado are not matched in any other setting suggesting $^{87}Sr/^{86}Sr$ is a good indicator of continental origin of formation fluids (see also discussion in Paytan et al., 2002; Widanagamage et al., 2015). Diagenetic barite (which precipitated in the subsurface from porewater) from Ocean Drilling Program Site 765 has relatively high $^{87}Sr/^{86}Sr$ (Table 1) indicating the presence of fluid impacted by terrigenous material within the interstitial waters.

3.4. Stable strontium isotopes

Stable Sr isotope measurements ($\delta^{88/86}$Sr) of marine hydrothermal samples and cold seep barites are indistinguishable and overlap with the range of $\delta^{88/86}$Sr values measured in continental spring barites (Fig. 3). Marine pelagic barite lies at the bottom of the range of values measured in the other marine environments but fall in the middle of the range of $\delta^{88/86}$Sr values measured in continental spring barites (Fig. 3). Therefore, while there is a range in isotope values, no distinct relationship is seen between stable Sr isotope measurements ($\delta^{88/86}$Sr) and the mode of formation (Table 2).

All barite samples are offset (fractionated) from the fluids in which they precipitate. The degree of isotopic fractionation for $\delta^{88/86}$Sr varies between and within a specific type of barite, except for marine pelagic barite which appears to have a consistent offset from seawater of approximately −0.53‰ in coretop samples from three different locations (Table 1). Two cold seep samples analyzed in this study from San Clemente Basin are also quite similar, but more locations are needed to assess whether the Sr isotopic composition of these types of barite are consistent between sites. Furthermore, the range of apparent isotopic fractionation within a particular setting where multiple sites have been measured is large (−0.6 to 0.0‰) except marine pelagic barite. Interestingly, hydrothermal barites with the lowest $^{87}Sr/^{86}Sr$ values indicative of a Sr source dominated by hydrothermal fluids (and little influence of seawater Sr) have the highest $\delta^{88/86}$Sr values compared to the other hydrothermal barite samples. The combination of the radiogenic and stable Sr isotope data suggests smaller stable Sr isotopic fractionations for these hydrothermal barites, whereas hydrothermal barite with more seawater-like $^{87}Sr/^{86}Sr$ values have larger stable Sr isotopic fractionations. The few cold seep and diagenetic barites that have been measured in this study appear to be dominated by seawater Sr and have stable Sr isotopic fractionations similar but not identical to marine pelagic barite.

The controls on Sr isotopic fractionation in all these settings except for the marine pelagic remain fairly unconstrained since there is no clear relationship with Sr in the water in these natural systems as previously concluded (Fig. 3a; Widanagamage et al., 2015). It was suggested that barite in the continental spring setting does not directly precipitate from solution, but heterogeneously within diverse microenvironments which influenced the isotopic fractionation of Sr possibly due to changes in saturation conditions, Sr concentrations and/or precipitation of other minerals like celestine, $SrSO_4$ (Widanagamage et al., 2015; Singer et al., 2016). This complicates any simple interpretation of $\delta^{88/86}$Sr for samples other than marine pelagic barite, which appears to form under more consistent conditions resulting in a constant offset from seawater. This new data supports conclusions drawn from stable calcium isotopes measurements of marine pelagic barite (Griffith et al., 2008).

It should be noted that even a highly stable sulfate mineral like barite could be susceptible to diagenetic reactions and variations in its stable isotopic composition within marine sediment formed during extreme climatic or environmental perturbations affecting the sediments post-deposition (e.g., ocean acidification at the Paleocene-Eocene Thermal Maximum; Griffith et al., 2015). Stable Ca isotopes appear to be sensitive to these diagenetic processes, whereas radiogenic Sr ratios are not (Griffith et al., 2015). It has been shown that the radiogenic Sr signature reflects the porewater composition dominated by seawater within the upper part of the sedimentary column, even where carbonate is rapidly dissolving (e.g., Fantle, 2015). Investigations of stable Sr isotopes are required to test whether this is also the case for stable Sr isotopes in barite and whether a combination of Ca and Sr stable isotopes measured on the same samples could shed light on processes dominating these isotope effects within marine sediments during extreme perturbations to these systems.

4. Conclusions

The combined use of the investigated metal and nonmetal isotopic measurements in barite could be useful to identify mode of barite mineralization for use in earth science applications including understanding ancient barite deposits. Characteristics of each barite formed in each setting described here are summarized in Table 2. Today, the major flux of Ba out of the oceans is thought to be marine pelagic barite formed in the water column associated with decaying organic matter (Paytan and Kastner, 1996). However, it is generally thought that this mode of barite formation was not dominant in the past when sulfate concentrations where much lower (e.g., Jamieson et al., 2013; Crowe et al., 2014), although recently this has been called into question (Horner et al., 2017). Future workers should carefully prepare and measure these geochemical parameters to test various hypotheses with this framework in mind but be cautioned that there is still a lot of work that can be done to better understand the various modern systems better and apply this knowledge to understand ancient barite deposits and potentially extraterrestrial systems. Additional detailed work using the isotopic composition of other elements, like barium, could help constrain the modern marine Ba cycle with hopes to better understand the past ocean (e.g., Horner et al., 2017; Hsieh and Henderson, 2017) and expand the existing metal isotopes useful for identifying the mode of barite formation.

Declarations of interest

None.

Acknowledgements

The authors would like to thank P. Lonsdale, M. Tivey, and D. Stakes for generously sharing their barite samples with us. Core samples from the Ocean Drilling Program were provide from the IODP Core Repositories. Coretop samples were provided by Scripps Institution of Oceanography and the Marine Geology Repository at Oregon State University. This work was funded in part by the National Science Foundation (NSF) EAR-1053312 to EMG, EAR-1053474 to HDS, and OCE-1259440 to AP. We would like to thank J. Senko and L. Krumholz for assistance in collecting samples in Oklahoma, and G. A. Briggs for granting us access to Doughty Springs, Colorado. The reviews of C. Pearce and an anonymous reviewer helped improve this revised manuscript.

References

Aharon, P., Fu, B., 2000. Microbial sulfate reduction rates and sulfur and oxygen isotope fractionations at oil and gas seeps in Deepwater Gulf of Mexico. Geochim. Cosmochim. Acta 64, 233–246.

AlKhatib, M., Eisenhauer, A., 2017. Calcium and strontium isotope fractionation in aqueous solutions as a function of temperature and reaction rate; I. Calcite. Geochim. Cosmochim. Acta 209, 296–319.

Antler, G., Turchyn, A.V., Rennie, V., Herut, B., Sivan, O., 2013. Coupled sulfur and oxygen isotope insight into bacterial sulfate reduction in the natural environment. Geochim. Cosmochim. Acta 118, 98–117.

Aquilina, L., Dia, A.N., Boulegue, J., Bourgois, J., Fouillac, A.M., 1997. Massive barite desposits in the convergent margin off Peru: implications for fluid circulation. Geochim. Cosmochim. Acta 61, 1233–1245.

Balci, N., Mayer, B., Shanks, W.C., Mandernack, K.W., 2012. Oxygen and sulfur isotope systematics of sulfate produced during abiotic and bacterial oxidation of sphalerite and elemental sulfur. Geochim. Cosmochim. Acta 77, 335–351.

Bertram, M.A., Cowen, J.P., 1997. Morphological and compositional evidence for biotic precipitation of marine barite. J. Mar. Res. 55, 577–593.

Bertram, M.A., Cowen, J.P., 1998. Biomineralization in agglutinating foraminifera: an analytical SEM investigation of external wall composition in three small test forms. Aquat. Geochem. 4, 455–468.

Böhlke, J.K., Mroczkowski, S.J., Coplen, T.B., 2003. Oxygen isotopes in nitrate: new reference materials for 18O:17O:16O measurements and observations on nitrate-water equilibration. Rapid Commun. Mass Spectrom. 17, 1835–1846.

Böttcher, M.E., Thamdrup, B., Vennemann, T.W., 2001a. Anaerobic sulfide oxidation and stable isotope fractionation associated with bacterial sulfur disproportionation in the

presence of MnO_2. Geochim. Cosmochim. Acta 65, 1573–1581.
Böttcher, M.E., Thamdrup, B., Vennemann, T.W., 2001b. Oxygen and sulfur isotope fractionation during anaerobic bacterial disproportionation of elemental sulfur. Geochim. Cosmochim. Acta 65, 1601–1609.
Böttcher, M.E., Thamdrup, B., Gehre, M., Theune, A., 2005. S-34/S-32 and O-18/O-16 fractionation during sulfur disproportionation by *Desulfobulbus propionicus*. Geomicrobiol J. 22, 219–226.
Bowen, G.J., Revenaugh, J., 2003. Interpolating the isotopic composition of modern meteoric precipitation. Water Resour. Res. 39 (10), 1299. https://doi.org/10.1029/2003WR002086.
Brabec, M.Y., Lyons, T.W., Mandernack, K.W., 2012. Oxygen and sulfur isotope fractionation during sulfide oxidation by anoxygenic phototrophic bacteria. Geochim. Cosmochim. Acta 83, 234–251.
Brand, W.A., Coplen, T.B., Aerts-Bijma, A.T., Böhlke, J.K., Gehre, M., Geilmann, H., Gröning, M., Jansen, H.G., Meijer, H.A.J., Mroczkowski, S.J., Qi, H., Soergel, K., Stuart-Williams, H., Weise, S.M., Werner, R.A., 2009. Comprehensive inter-laboratory calibration of reference materials for $\delta^{18}O$ versus VSMOW using various on-line high-temperature conversion techniques. Rapid Commun. Mass Spectrom. 23, 999–1019.
Breit, G.N., Simmons, E.C., Goldhaber, M.B., 1985. Dissolution of barite for the analysis of strontium isotopes and other chemical and isotopic variations using aqueous sodium carbonate. Chem. Geol. 52 (3–4), 333–336.
Brunner, B., Bernasconi, S.M., 2005. A revised isotope fractionation model for dissimilatory sulfate reduction in sulfate reducing bacteria. Geochim. Cosmochim. Acta 69 (20), 4759–4771.
Brunner, B., Bernasconi, S.M., Kleikemper, J., Schroth, M., 2005. A model for oxygen and sulfur isotope fractionation in sulfate during bacterial sulfate reduction processes. Geochim. Cosmochim. Acta 69 (20), 4773–4785.
Chiba, H., Sakai, H., 1985. Oxygen isotope exchange rate between dissolved sulfate and water at hydrothermal temperatures. Geochim. Cosmochim. Acta 49, 993–1000.
Claypool, G.E., Holser, W.T., Kaplan, I.R., Sakai, H., Zak, I., 1980. The age curves of sulfur and oxygen isotopes in marine sulfate and their mutual interpretation. Chem. Geol. 28, 199–260.
Coplen, T.B., Hopple, J.A., Böhlke, J.K., Peiser, H.S., Rieder, S.E., Krouse, H.R., Rosman, K.J.R., Ding, T., Vocke, R.D.Jr., Révész, K.M., Lamberty, A., Taylor, P., De Bièvre, P., 2001. Compilation of minimum and maximum isotope ratios of selected elements in naturally occurring terrestrial materials and reagents. Water Resour. Invest. Rep. U.S. Geol. Surv. 01–4222.
Crowe, S.A., Paris, G., Katsev, S., Jones, C., Kim, S.-T., Zerkle, A.L., Nomosatryo, S., Fowle, D.A., Adkins, J.F., Sessions, A.L., Farquhar, J., Canfield, D.E., 2014. Sulfate was a trace constituent of Archean seawater. Science 346, 735–739.
Dansgaard, W., 1964. Stable isotopes in precipitation. Tellus 16, 436–468.
Deusner, C., Holler, T., Arnold, G.L., Bernasconi, S.M., Formolo, M.J., Brunner, B., 2014. Sulfur and oxygen isotope fractionation during sulfate reduction coupled to anaerobic oxidation of methane is dependent on methane concentration. Earth Planet. Sci. Lett. 399, 61–73. https://doi.org/10.1016/j.epsl.2014.04.047.
Eickmann, B., Thorseth, I.H., Peters, M., Strauss, H., Brocker, M., Pedersen, R.B., 2014. Barite in hydrothermal environments as a recorder of subseafloor processes: a multiple-isotope study from the Loki's Castle vent field. Geobiology 12, 308–321.
Elsgaard, M.F., Jorgensen, B.B., Alayse, A.M., Jannasch, H.W., 1994. Microbial sulfate reduction in deep-sea sediments at the Guaymas Basin hydrothermal vent area: influence of temperature and substrates. Geochim. Cosmochim. Acta 58, 3335–3343.
Elshahed, M.S., Senko, J.M., Dewers, T.A., Spear, J.R., Najar, F.Z., Kenton, S.M., Roe, B.A., Krumholz, L.R., 2003. Bacterial diversity and sulfur cycling in a mesophilic sulfide-rich spring. Appl. Environ. Microbiol. 69, 5609–5621.
Fantle, M.S., 2015. Calcium isotopic evidence for rapid recrystallization of bulk marine carbonates and implications for geochemical proxies. Geochim. Cosmochim. Acta 148, 378–401.
Feng, D., Roberts, H., 2011. Geochemical characteristics of the barite deposits at cold seeps from the northern Gulf of Mexico. Earth Planet. Sci. Lett. 309, 89–99.
Fietzke, J., Eisenhauer, A., 2006. Determination of temperature-dependent stable strontium isotope (88Sr/86Sr) fractionation via bracketing standard MC-ICP-MS. Geochem. Geophys. Geosyst. 7 (8). https://doi.org/10.1029/2006GC001243.
Finlay, B.J., Hetherington, N.B., Da Vison, W., 1983. Active biological participation in lacustrine barium chemistry. Geochim. Cosmochim. Acta 47, 1325–1329.
Fritz, P., Basharmal, G.M., Drimmie, R.J., Ibsen, J., Qureshi, R.M., 1989. Oxygen isotope exchange between sulphate and water during bacterial reduction of sulphate. Chem. Geol. 79, 99–105.
Gill, B.C., Lyons, T.W., Saltzman, M.R., 2007. Parallel, high- resolution carbon and sulfur isotope records of the evolving Paleozoic marine sulfur reservoir. Palaeogeogr. Palaeoclimatol. Palaeoecol. 256, 156–173.
González-Muñoz, M.T., Fernandez-Luque, B., Martinez-Ruiz, F., Ben Chekroun, K., Arias, J.M., Rodriguez-Gallego, M., Martinez-Canamero, M., de Linares, C., Paytan, A., 2003. Precipitation of barite by *Myxococcus xanthus*: possible implications for the biogeochemical cycle of barium. Appl. Environ. Microbiol. 69, 5722–5725. https://doi.org/10.1128/AEM.69.9.5722-5725.2003.
González-Múñoz, M.T., Martinez-Ruiz, F., Martin-Ramos, J.D., Paytan, A., 2012. Precipitation of barite by marine bacteria: a possible mechanism for marine barite formation. Geology 40, 675–678.
Gooday, A.J., Nott, J.A., 1982. Intracellular barite crystals in two Xenophyaphores, Aschemonella Ramuliformis and Galatheammina Sp. with comments on the taxonomy of A. Ramuliformis. J. Mar. Biol. Assoc. UK 62, 595–605.
Goodfellow, W.D., Grapes, K., Cameron, B., Franklin, J.M., 1993. Hydrothermal alteration associated with massive sulfide deposits, Middle Valley, northern Juan de Fuca Ridge. Can. Mineral. 31, 1025–1060.
Greinert, J., Bollwerk, S.M., Derkachev, A., Bohrmann, G., Suess, E., 2002. Massive barite deposits and carbonate mineralization in the Derugin Basin, Sea of Okhotsk: precipitation processes at cold seep sites. Earth Planet. Sci. Lett. 203, 165–180.
Griffith, E.M., Paytan, A., 2012. Barite in the ocean—occurrences, geochemistry and paleoceanographic applications. Sedimentology 59 (6), 1817–1835.
Griffith, E.M., Schauble, E.A., Bullen, T.D., Paytan, A., 2008. Characterization of calcium isotopes in natural and synthetic barite. Geochim. Cosmochim. Acta 72, 5641–5658.
Griffith, E.M., Fantle, M.S., Eisenhauer, A., Paytan, A., Bullen, T.D., 2015. Effects of ocean acidification on the marine calcium isotope record at the Paleocene-Eocene Boundary. Earth Planet. Sci. Lett. 419, 81–92.
Hannington, M.D., Scott, S.D., 1988. Mineralogy and geochemistry of a hydrothermal silica-sulfide-sulfate spire in the caldera of Axial-Seamount, Juan de Fuca Ridge. Can. Mineral. 26, 603–625.
Harrison, A., Thode, H.G., 1958. Mechanism of the bacterial reduction of sulphate from isotope fractionation studies. Trans. Faraday Soc. 54, 84–92.
Horner, T.J., Pryer, H.V., Nielsen, S.G., Crockford, P.W., Gauglitz, J.M., Wing, B.A., Ricketts, R.D., 2017. Pelagic barite precipitation at micromolar ambient sulfate. Nat. Commun. 8, 1342. https://doi.org/10.1038/s41467-017-01229-5.
Hsieh, Y.-T., Henderson, G.M., 2017. Barium stable isotopes in the global ocean: tracer of Ba inputs and utilization. Earth Planet. Sci. Lett. 473, 269–278.
Jamieson, J.W., Wing, B.A., Farquhar, J., Hannington, M.D., 2013. Neoarchaean seawater sulphate concentrations from sulphur isotopes in massive sulphide ore. Nat. Geosci. 6, 61–64.
Jennings, D.S., Driese, S.G., 2014. Understanding barite and gypsum precipitation in upland acid-sulfate soils: an example from a Lufkin Series toposequence, south-central Texas, USA. Sediment. Geol. 299, 106–118.
Johnston, D.T., Gill, B.C., Masterson, A., Beirne, E., Casciotti, K.L., Knapp, A.N., Berelson, W., 2014. Placing an upper limit on cryptic marine sulphur cycling. Nature 514 (7519), 530–533.
Kim, J., Lee, I., Lee, K.-Y., 2004. S, Sr, and Pb isotopic systematics of hydrothermal chimney precipitates from the Eastern Manus Basin, western Pacific: evaluation of magmatic contribution to hydrothermal system. J. Geophys. Res. 109, B12210. https://doi.org/10.1029/2003JB002912.
Koski, R.A., Hein, J.R., 2003. Stratiform barite deposits in the Roberts Mountains allochthon, Nevada: a review of potential analogs in modern sea-floor environments. U.S. Geol. Surv. Bull. 2209-H (17 p).
Krabbenhöft, A., Fietzke, J., Eisenhauer, A., Liebetrau, V., Böhm, F., Vollstaedt, H., 2009. Determination of radiogenic and stable strontium isotope ratios ($^{87/86}Sr$; $\delta^{88/86}Sr$) by thermal ionization mass spectrometry applying an $^{87/84}Sr$ double spike. J. Anal. At. Spectrom. 24 (9), 1267–1271.
Krabbenhöft, A., Eisenhauer, A., Böhm, F., Vollstaedt, H., Fietzke, J., Liebetrau, V., Augustin, N., Peucker-Ehrenbrink, B., Muller, M.N., Horn, C., Hansen, B.T., Nolte, N., Wallmann, K., 2010. Constraining the marine strontium budget with natural strontium isotope fractionations ($^{87}Sr/^{86}Sr^{*}$, $\delta^{88/86}Sr$) of carbonates, hydrothermal solutions and river waters. Geochim. Cosmochim. Acta 74, 4097–4109.
Kramchaninov, A.Y., Chernyshev, I.V., Shatagin, K.N., 2012. Isotope analysis of strontium by multicollector inductively-coupled plasma mass spectrometry: high-precision combined measurements of $^{88}Sr/^{86}Sr$ and $^{87}Sr/^{86}Sr$ isotope ratios. J. Anal. Chem. 67, 1084–1092.
Kroopnick, P., Craig, H., 1972. Atmospheric oxygen: isotopic composition and solubility fractionation. Science 175, 54–55.
Kusakabe, M., Robinson, B.W., 1977. Oxygen and sulfur isotope equilibria in the BaSO4-H2SO4-H2O system from 110 to 350 °C and applications. Geochim. Cosmochim. Acta 41, 1033–1040.
Markovic, S., Paytan, A., Li, H., Wortmann, U.G., 2016. A revised seawater sulfate oxygen isotope record for the last 4 Myr. Geochim. Cosmochim. Acta 175, 239–251.
Martinez-Ruiz, F., Jroundi, F., Paytan, A., Guerra-Tschuschke, I., del Mar Abad, M., González-Muñoz, M.T., 2018. Barium bioaccumulation by bacterial biofilms and implications for Ba cycling and use of Ba proxies. Nat. Commun. 9, 1619. https://doi.org/10.1038/s41467-018-04069-z.
Maynard, J.B., Morton, J., Valdes-Nodarse, E.L., Diaz-Carmona, A., 1995. Sr isotopes of bedded barites: guide to distinguishing basins with Pb–Zn mineralization. Econ. Geol. 90, 2064–2085.
Nier, A.O., 1938. The isotopic constitution of strontium, barium, bismuth, thallium and mercury. Phys. Rev. 5, 275–278.
Paytan, A., Kastner, M., 1996. Benthic Ba fluxes in the central Equatorial Pacific, implications for the oceanic Ba cycle. Earth Planet. Sci. Lett. 142, 439–450.
Paytan, A., Kastner, M., Martin, E.E., Macdougall, J.D., Herbert, T., 1993. Marine barite as a monitor of seawater strontium isotope composition. Nature 366, 445–449.
Paytan, A., Kastner, M., Campbell, D., Thiemens, M.H., 1998. Sulfur isotopic composition of Cenozoic seawater sulfate. Science 282, 1459–1462.
Paytan, A., Mearon, S., Cobb, K., Kastner, M., 2002. Origin of marine barite deposits: Sr and S isotope characterization. Geology 30, 747–750.
Paytan, A., Kastner, M., Campbell, D., Thiemens, M.H., 2004. Seawater sulfur isotope fluctuations in the Cretaceous. Science 304, 1663–1665.
Pearce, C.R., Parkinson, I.J., Gaillardet, J., Charlier, B.L.A., Mokadem, F., Burton, K.W., 2015. Reassessing the stable (δ88/86Sr) and radiogenic (87Sr/86Sr) strontium isotopic composition of marine inputs. Geochim. Cosmochim. Acta 157, 125–147.
Rees, C.E., 1973. A steady-state model for sulphur isotope fractionation in bacterial reduction processes. Geochim. Cosmochim. Acta 37 (5), 1141–1162.
Reesman, R.H., 1968. Rb-Sr analyses of some sulfide mineralization. Earth Planet. Sci. Lett. 5, 23–26.
Sanz-Montero, M.E., Rodriguez-Aranda, J.P., Garcia del Cura, M.A., 2009. Bioinduced precipitation of barite and celestite in dolomite microbalites: examples from Miocene lacustrine sequences in the Madrid and Duero Basins, Spain. Sediment. Geol. 222, 138–148.
Scher, H.D., Griffith, E.M., Buckley Jr., W.B., 2014. Accuracy and precision of 88Sr/86Sr

and 87Sr/86Sr measurements by MCICPMS compromised by high barium concentrations. Geochem. Geophys. Geosyst. https://doi.org/10.1002/2013GC005134.
Seal, I., Robert, R., Alpers, C.N., Rye, R.O., 2000. Stable isotope systematics of sulfate minerals. In: Alpers, C.N., Jambor, J.L., Nordstrom, D.K. (Eds.), Sulfate Minerals: Crystallography, Geochemistry, and Environmental Significance. Reviews in Mineralogy and Geochemistry Mineralogical Society of America, Washington D.C., pp. 541–602.
Senko, J.M., Campbell, B.S., Henriksen, J.R., Elshahed, M.S., Dewers, T.A., Krumholz, L.R., 2004. Barite deposition resulting from phototrophic sulfide-oxidizing bacterial activity. Geochim. Cosmochim. Acta 68 (4), 773–780.
Singer, D.M., Griffith, E.M., Senko, J.M., Fitzgibbon, K., Widanagamage, I.H., 2016. Celestine in a sulfidic spring barite deposit – a potential biomarker? Chem. Geol. 440, 15–25.
Smith, E., Hamilton, J., Davison, T., Fullwood, N.J., McGrath, M., 2004. The effect of humic substances on barite precipitation–dissolution behavior in natural and synthetic lake waters. Chem. Geol. 207 (1–2), 81–89.
Stevens, E.W.N., Bailey, J.V., Flood, B.E., Jones, D.S., Gilhooly III, W.P., Joye, S.B., Teske, A., Mason, O.U., 2015. Barite encrustation of benthic sulfur-oxidizing bacteria at a marine cold seep. Geobiology 13 (6), 588–603.
Taylor, B.E., Wheeler, M.C., Nordstrom, D.K., 1984. Isotope composition of sulphate in acid mine drainage as measure of bacterial oxidation. Nature 308, 538–541.
Torres, M.E., Bohrmann, G., Dube, T.E., Poole, F.G., 2003. Formation of modern and Paleozoic stratiform barite at cold methane seeps on continental margins. Geology 31, 897–900.
Turchyn, A.V., Schrag, D.P., 2004. Oxygen isotope constraints on the sulfur cycle over the past 10 million years. Science 303, 2004–2007.
Turchyn, A.V., Schrag, D.P., 2006. Cenozoic evolution of the sulfur cycle: insight from oxygen isotopes in marine sulfate. Earth Planet. Sci. Lett. 241, 763–779.
Turchyn, A.V., Bruchert, V., Lyons, T.W., Engel, G.S., Balci, N., Schrag, D.P., Brunner, B., 2010. Kinetic oxygen isotope effects during dissimilatory sulfate reduction: a combined theoretical and experimental approach. Geochim. Cosmochim. Acta 74, 2011–2024.
Van Stempvoort, D.R., Krouse, H.R., 1994. Controls of d18O in sulfate review of experimental data and application to specific environments. In: Alpers, C.N., Blowes, D.W. (Eds.), Environmental Geochemistry of Sulfide Oxidation. ACS Symposium Series, vol. 550. American Chemical Society, Washington, D.C., pp. 446–480.
Veizer, J., Ala, D., Azmy, K., Bruckschen, P., Buhl, D., Bruhn, F., Cargen, G.A.F., Diener, A., Ebneth, S., Godderis, Y., Jasper, T., Korte, C., Pawellek, F., Podlaha, O.G., Strauss, H., 1999. 87Sr/86Sr, δ13C and δ18O evolution of Phanerozoic seawater. Chem. Geol. 161, 59–88.
Widanagamage, I.H., Schauble, E.A., Scher, H.D., Griffith, E.M., 2014. Stable strontium isotope fractionation in synthetic barite. Geochim. Cosmochim. Acta 140, 58–75.
Widanagamage, I.H., Griffith, E.M., Singer, D.M., Scher, H.D., Buckley, W.P., Senko, J.M., 2015. Controls on stable Sr-isotope fractionation in continental barite. Chem. Geol. 411, 215–227.
Wing, B.A., Halevy, I., 2014. Intracellular metabolite levels shape sulfur isotope fractionation during microbial sulfate respiration. PNAS 111 (51), 18116–18125.
Wortmann, U.G., Paytan, A., 2012. Rapid variability of seawater chemistry over the past 130 million years. Science 337 (6092), 334–336.
Wortmann, U.G., Bernasconi, S.M., Böttcher, M.E., 2001. Hypersulfidic deep biosphere indicates extremem sulfur isotope fractionation during single-step microbial sulfate reduction. Geology 29 (7), 647–650.
Wortmann, U.G., Chernyavsky, B., Bernasconi, S.M., Brunner, B., Böttcher, M.E., Swart, P.K., 2007. Oxygen isotope biogeochemistry of pore water sulfate in the deep biosphere: dominance of isotope exchange reactions with ambient water during microbial sulfate reduction (ODP Site 1130). Geochim. Cosmochim. Acta 71, 4221–4232.
Zak, I., Sakai, H., Kaplan, I.R., 1980. Factors controlling the 18O/16O and 34S/32S isotope ratios of ocean sulfates, evaporites and interstitial sulfates from modern deep sea sediments. In: Goldberg, E.D. (Ed.), Isotope Marine Chemistry. Geochemistry Research Association, pp. 339–373 Chap. 17.